J Mater Sci (2008) 43:927–932
DOI 10.1007/s10853-007-2206-5

The relationship between activation energy and precipitate size for precipitate agglomeration

Ercan Balikci · Aravamudhan Raman

Received: 15 May 2007 / Accepted: 4 October 2007 / Published online: 9 November 2007

Abstract Superalloys are used in aggressive atmospheres in aero-engines and land-base gas turbines. IN738LC is an important superalloy used in gas turbines. Strengthening $Ni_3(Al,Ti,Nb)$ type precipitate phase in this superalloy goes through size and morphological changes with time and temperature. Experimental observations suggest precipitate motion as a whole in the matrix leading to agglomeration of nearby precipitates for coarsening, which is in contrast to the traditional Ostwald ripening. Likewise, contrary to the conventionally accepted view of constant activation energy, experimental data in this study indicate varying activation energy, which causes coalescence and relates to the precipitate size in the form of an increasing polynomial.

Introduction

Superalloys are employed in aggressive atmospheres in aero-engines and land-base gas turbines. Their prime candidacy for such applications is due to good corrosion resistance, optimal thermal properties, strength coupled with ductility, creep and fatigue resistance, and optimal impact/wear resistance. The unique set of properties in these alloys is due to an fcc Ni-base solid solution matrix which is hardened by solutes, carbides, and precipitates of $Ni_3(Al,Ti)$ intermetallic compounds.

E. Balikci (✉)
Department of Mechanical Engineering, Bogazici University, South Campus, 34342 Istanbul, Turkey
e-mail: ercan.balikci@boun.edu.tr

A. Raman
Department of Mechanical Engineering, Louisiana State University, Baton Rouge, LA 70803, USA

IN738LC is an important superalloy used mainly in land-base gas turbines for electricity production. A limited number of publications on this superalloy indicates the necessity of controlling the microstructure, which strictly determines the physical and mechanical properties [1–7]. In this alloy, precipitates form in spherical shape, which later coarsen to a cubical shape dictated by anisotropic elastic properties and surface energy. The unimodal cuboidal form is sustained up to about 700 nm size after which a bimodal precipitate distribution is observed [8–15].

A number of experimental and theoretical studies have been carried out to explore the coarsening features of the second phase precipitate particles [16–43]. Various investigators considered the coarsening behavior of positively or negatively misfitting precipitates in the matrix. Precipitate evolution progresses toward the minimization of the total free energy of the system, which has two contributing factors: the interfacial surface energy and the elastic strain energy. Results have suggested that the elastic strain energy due to the elastic self-energy and the configurational energy of the particles could play an effective role during the coarsening of precipitates. At the early stages of coarsening, the interfacial energy dominates the morphological evolution, while after the precipitates reach a critical size, the elastic strain energy term takes over. Directional alignment of the coarsening precipitates along the elastically soft directions, <100> in the Ni alloy systems, has also been reported, and it has again been attributed to the tendency to minimize the free energy of the system.

Coarsening of precipitates takes place in constant precipitate volume following the growth period, during which precipitate volume increases by solute absorption from the matrix. Conventionally, activation energy for precipitate size change (growth/coarsening) is constant in a given temperature range and appears in the well-known Arhenius

equation. Constant activation energy indicates that no mechanism change occurs for the process under consideration. However, such variations in the microstructure, as dislocation configuration and strain field surrounding the precipitate particles, encourage suggesting a varying, precipitate size dependent activation energy based on the experimental precipitate size measurements that will be provided in the following sections. Hence, in this current work, coalescence of precipitates is investigated to propose a relationship between the activation energy and precipitate size.

Experimental

The material used in this study was the polycrystalline IN738LC superalloy provided by Howmet Corporation, Whitehall, Michigan, in the form of rods with 15 mm diameter and 110 mm length in HIPed (hot isostatic pressed) condition whose microstructure is shown in Fig. 1. Various solution and aging heat treatments were carried out under vacuum to observe precipitate microstructure evolution. After the heat treatments, precipitate microstructure analysis started with conventional metallographic sample preparation, and then continued with Scanning Electron Microscop (SEM) (Hitachi S-2460N) observations. Chemical etching was performed using a solution of 33% HNO_3 + 33% acetic acid + 33% H_2O + 1% HF. Precipitate size and volume fraction in the various conditions were measured from the SEM micrographs in a McIntosh® computer using the Prism View Image Analysis & Measurement program (ImageSet™) by Dapple Systems, Inc., Sunnyvale, CA.

Results and discussions

Precipitate microstructure evolution in the superalloy IN738LC has been extensively studied and reported in several publications by the authors of this current article [8–15]. Only the relevant data will be reported here to explore the features of precipitate coarsening. Precipitate sizes measured from the SEM micrographs, given in Table 1, show coarsening with increased temperature. Precipitate volume stays constant.

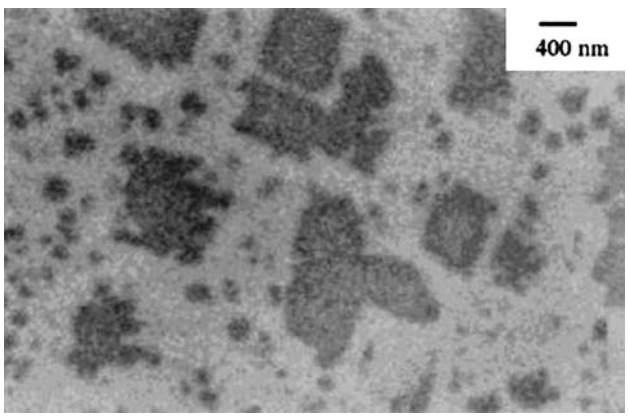

Fig. 1 Precipitate microstructure of as received IN738LC. Small and large dark features are precipitates

Precipitates generally coarsen by picking up from the matrix the solute atoms of dissolved small size precipitates, driven by the atomic diffusion process. Nevertheless, the features shown in Fig. 2 are clearly indicative of the fact that the precipitate coarsening is not controlled by conventional atomic diffusion process, wherein the smaller precipitates dissolve into the matrix, the solute atoms diffuse toward the larger ones, and their absorption by the latter leads to the precipitate coarsening due to the familiar Gibbs-Thompson effect. This process, Ostwald ripening, has been studied widely [19–23]. Although this process may be occurring, the precipitate coarsening illustrated in Fig. 2 is via the agglomeration (consolidation) of adjacent precipitates. This process can still be considered as activated by interdiffusion of atoms at the interface leading to its migration in the direction of possible attractive force activating the migration of the precipitate as a whole in the matrix medium.

The precipitate movement in the matrix as a whole for agglomeration purposes has been proposed previously [16] where the closely spaced precipitates have been suggested to move toward each other and join by the removal of elastically strained matrix. Voorhees and Johnson [17] has theoretically analyzed the particle migration in the matrix driven by the elastic stresses. They basically have derived the formulae for growth rate and migration velocity of the mass center of precipitates, considering the elastic energies. Others also have considered the coalescence process by taking into account the lattice misfit, the applied stress, and the elastic properties of the constituent phases in the system [19, 24–43]. General finding is that the sign of the misfit and the applied stress, the ratio of the elastic properties of the precipitate and the matrix phase, and the interfacial energy might significantly affect the precipitate evolution. Also, some of the results indicate an inverse coarsening [24–26], where smaller precipitates may grow at the expense of the larger ones due to the elastic interactions between the precipitates. This finding, which is quite the opposite of the conventional view, also contradicts the growth mode by Ostwald ripening.

The particle motion can be conceived to be due to the pull out of the face of the particles in the direction of attractive force acting between the merging precipitates and corresponding caving-in at the opposite tail end of the particle. The advancing front can be projected to be pulled out by activating the diffusion of the solute atoms from the precipitates into the adjoining matrix planes at the

Table 1 Size of the γ' precipitates in water quenched conditions after aging for 24 h subsequent to solutionizing at 1,200 °C, which yields a unimodal size of ~70 nm precipitates

Aging temperature, °C	850	950	1,050	1,070	1,090	1,120	1,140	1,200
Precipitate size, nm	112	187	315	395	468	655	622	70
	(1,080)	(430)	(135)	(72)	(58)	(32)	(28)	(1,800)
	[−6/+10]	[−19/+10]	[−14/+18]	[−25/+15]	[−20/+22]	[−25/+10]	[−22/+25]	[±3]

First line in each data cell gives the average precipitate size, second line number of precipitate particles averaged, and third line % deviation in size of the precipitates. Number of precipitates is given in a 4 × 5 in.^{2} area

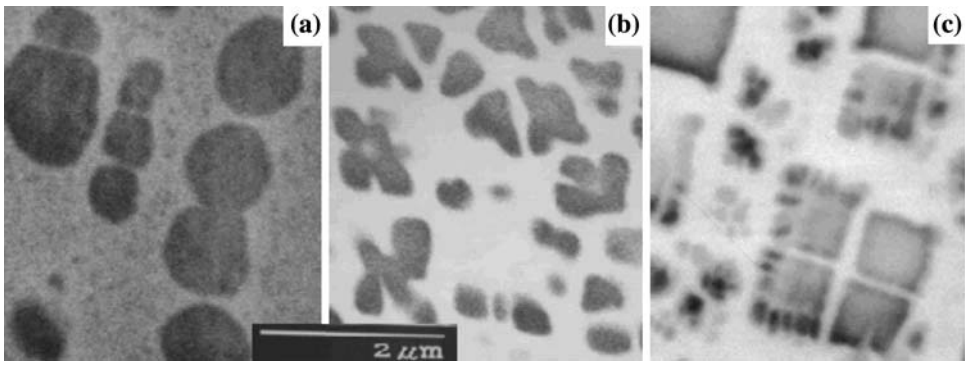

Fig. 2 SEM micrographs showing coalescence of precipitates (**a**) at 1,140 °C, (**b**) at 1,200 °C, (**c**) at 1,120°C

interface. The matrix layers in contact with the interface are then projected to slowly convert to precipitate layers. Simultaneously, diffusion of the solvent atoms from the matrix layers into the precipitate layers at the interface occurring at the opposite tail end would convert the precipitate layers into the matrix. This mechanism could possibly be aided by the vacancy and/or dislocation concentration at the interface. Removal of the elastically strained matrix between the merging precipitates also positively contributes to the process.

Another equally possible mechanism for particle motion is that a slight Poisson's contraction of the precipitates at the surfaces perpendicular to the moving front allows diffusion of the solvent atoms into these contracted surfaces. This would enable the removal of the squeezed-in matrix between the moving (joining) particles, and its readjustment at the faces and the tail end of the moving precipitates. Concurrently, the deformed precipitates should readjust their shape to cuboidal form, requiring the solute redistribution in the distorted precipitates during and after the consolidation.

Following sections describe the procedure to establish a relationship between the activation energy and precipitate size. To calculate the activation energy for the coalescence of the precipitates, slope of log (d) vs. $1/T$ plot is employed, where d is precipitate size and T is temperature. The ultimate aim is to better understand and define the nature of the activation energy required to coalesce the precipitates. The absence of any such study in the literature, to the authors' knowledge, makes this analysis significant, although attempts have been made earlier to formulate the minimum energy configurations for precipitates during directional alignment [30, 36, 37].

Assuming linear variation of log (d) vs. $1/T$ in different temperature ranges, the activation energy for the precipitate coalescence, Q, is calculated by segmenting the plot of log (d) vs. $1/T$, shown in Fig. 3, into three parts (850–950 °C, 950–1,050 °C, and 1,050–1,120 °C), and three different activation energies are obtained from the slopes of these segments by utilizing the Arhenius type growth equation:

$$d^{\mathrm{n}} - d_{\mathrm{o}}^{\mathrm{n}} = Ate^{-Q/RT} \tag{1}$$

Here, d_{o} is the initial precipitate size, A is a preexponential constant, t is aging time, and R is the gas constant. The segmenting is performed in small temperature intervals where a change in slope is seen. As Q is traditionally constant in a temperature range, this procedure is consistent with the well-established scientific knowledge. An additional activation energy value is calculated for the aging treatment at 1,140 °C. In order to calculate this additional activation energy value at 1,140 °C, the A value in the growth equation needs to be known in advance. After calculating the activation energy in the range 1,050–1,120 °C and inserting this activation energy value back in Eq. 1, the value for A is obtained. Use of the A value calculated from the data in the range 1,050–1,120 °C for the activation energy calculation at 1,140 °C is a reasonable approximation, since 1,140 °C is in the vicinity of this temperature range. Plot of the four calculated activation energies mentioned above for precipitate growth vs.

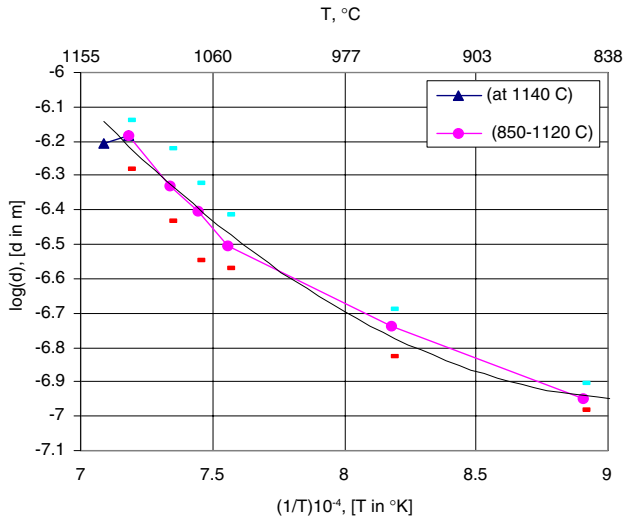

Fig. 3 Plot of log(d) vs. $1/T$ of γ' size. Black (thin) continues curve is best fit to the experimental size data

average temperature in the various temperature ranges is shown in Fig. 4. A best curve fit to the experimental data points for Q varying with T showed a polynomial form as follows:

$$Q(T) = (2.3356\text{e-}8)T^4 - (9.313\text{e-}5)T^3 + (0.1382)T^2 - (90.398)T + 22175 \quad (2)$$

Traditionally, the activation energy, Q, which is the energy needed to initiate a process, is assumed to be constant for a temperature range as appears in the Arhenius equation. However, here an increasing polynomial dependency of Q on T is obtained. The continuously increasing activation energy for precipitate growth with increasing temperature is an interesting observation. Even higher activation energies have been reported [8, 9, 14] for higher temperatures in the range 1,150–1,225 °C (e.g., 817 kJ/mol for the precipitate growth at 1,160 °C), indicating sluggish growth at high temperatures and signaling the dissolution of precipitates.

The next attempt is to correlate the activation energy to the precipitate size and the interprecipitate spacing. It is seen from the data in Table 1 and as displayed in Fig. 5 that the size of the precipitates varies as a polynomial function of T, given as follows:

$$d_{cf}(T) = (3.30779\text{e-}5)T^3 - (0.116511)T^2 + (137.333)T - 54021.6 \quad (3)$$

In the equations and figure legends hereafter, cf stands for curve fit, c for calculated, and m for measured. Interprecipitate spacing was measured and also calculated employing the sketch in Fig. 6 and Eq. 4 [44]:

$$s = \left(\sqrt{1/A_f} - 1\right) d \quad (4)$$

where s is the spacing between adjacent particles and A_f the area fraction. A proportional dependence of s with d can be seen in Fig. 7, which indicates that the interprecipitate spacing increases with increasing size of the precipitates (constant volume). This means that the increased size of the precipitates and the increased spacing between the adjacent ones necessitate more energy to coalesce them for growth. The increasing activation energy with increasing precipitate size and interparticle spacing is illustrated in Fig. 8. The Q_{cf} values are the activation energy values calculated using Eq. 2 at different temperatures, which yielded the corresponding precipitate size and interparticle spacing.

The "Precipitate Agglomeration Model (PAM)":

The requirement for more energy for the coalescence process could be better understood when a clear distinction between the processes for the growth is made; one via disintegration or dissolution followed by atomic diffusion and the other by coalescence (i.e., by the movement of

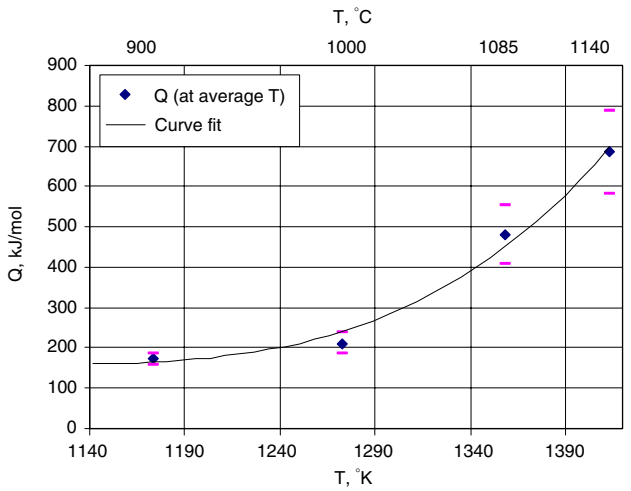

Fig. 4 Plot of Q vs. T

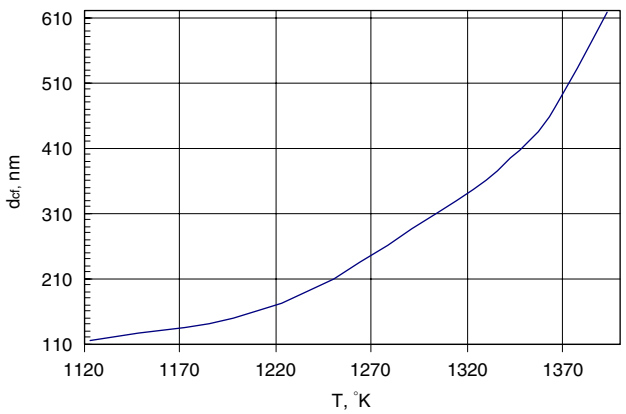

Fig. 5 d_{cf} vs. T. d_{cf} values were obtained by best curve fit to experimental data presented in Table 1 and Fig. 3

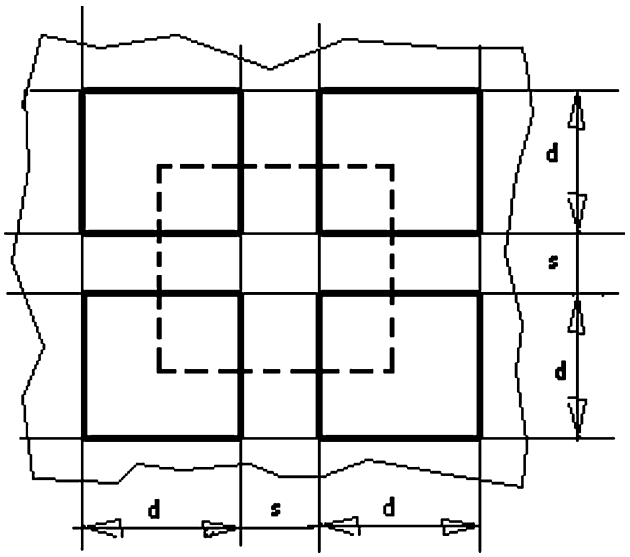

Fig. 6 Evenly distributed cuboidal precipitates in the matrix. The dashed line shows the unit cell used to calculate the spacing (s) between the precipitates

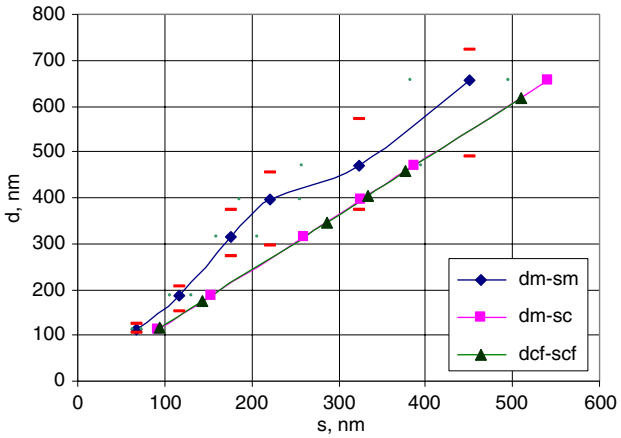

Fig. 7 Plot of d vs. s

particles as a whole). In the latter, since the whole particle needs to move, it could be deduced that larger the size and more the distance to be moved, the more energy it would require.

Based on the above presentation, a simple 'Precipitate Agglomeration Model (PAM)' is proposed. It is postulated that the consolidation of adjacent particles by particle motion is due to an attractive force F_A exerted by the particles on one another. This attractive force is conceived to develop by the need to reduce the overall surface interfacial energy of the precipitates and to lower the elastic strain energy by removal of the strained matrix between the joining precipitates. The surface area of the particle is a function of the size 'd' of the particle and should be proportional to d^2. Hence, one can write:

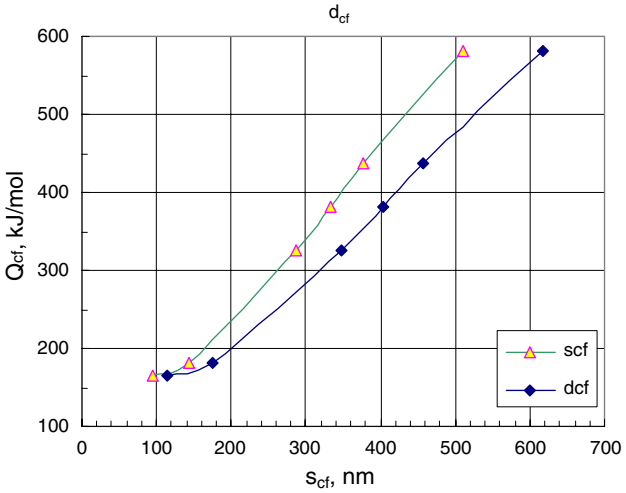

Fig. 8 Plot of Q_{cf} vs. d_{cf} and s_{cf}

$$F_A = f(d^2), \text{ where '}d\text{' is a function of temperature} \quad (5)$$

The particles are drawn toward each other by F_A and coalesce. Hence, the agglomeration energy can be postulated to be a function of the product of the attractive force and the interprecipitate distance s. Since the interprecipitate spacing is linearly proportional to the precipitate size, as indicated in Eq. 4 and seen in Fig. 7, the following can be suggested.

$$Q(d) \propto (F_A)s \propto f(d^2)f(d) \propto f(d^3) \quad (6)$$

Q_{cf} values obtained for the d_{cf} values of Fig. 3, plotted in Fig. 8, are again replotted against d_{cf}^3, which is shown in Fig. 9. The function governing the curve shown in this plot is determined to be a polynomial given below:

$$Q = (4.96634\text{e-}23)(d^3)^3 - (2.57128\text{e-}14)(d^3)^2 + (5.11797\text{e-}6)(d^3) + 155 \quad (7)$$

This function represents an increasing dependency of Q to d^3 (i.e., to volume and hence, to mass of each particle), and represents the variation of Q with the coarsening of the particles. Similar trend is seen in Fig. 8, too. Thus, it can be inferred that the agglomeration or consolidation energy is dependent on a function of the volume or the mass of the consolidating particles. Equation 7 is a function coming out of the experimental data. Further definition and refinement of the agglomeration energy is possible in future attempts.

It is reported [33] that coarsening slows down at high magnitude of the misfit, since the elastic strains are proportional to the square of the misfit. This means that precipitates with larger sizes, having higher misfit and elastic strains, would not favor the growth, and more energy supply would be required to advance any further coarsening. Likewise, PAM proposes that the consolidation

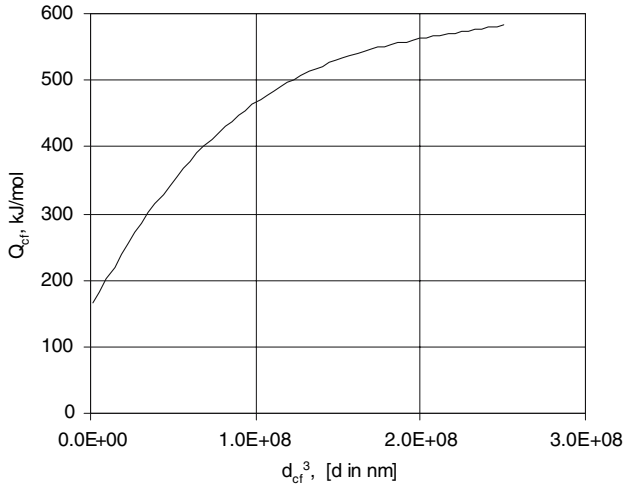

Fig. 9 Plot of Q_{cf} vs. d_{cf}^3

(activation) energy is a function of d^3. It may be possible in further attempts to define the attractive force F_A in terms of interfacial surface energy and elastic property differences between the matrix phase and the precipitates, and to devise a better system of equations based on the premises of precipitate agglomeration model proposed here in this article.

Conclusions

Precipitate agglomeration is observed to be via merging of nearby precipitates as a whole in contrast to conventional Ostwald ripening. Analysis of experimentally determined precipitate size data shows that activation energy is proportional to the size and hence, the mass of the precipitates, and it increases with increased precipitate size and inter-precipitate spacing.

References

1. Bieber CG, Suffern, Galka JJ (1969) United States Patent Office, No: 3459545, August 1969
2. Mukherji D, Jiao F, Chen W, Wahi RP (1991) Acta Metall Mater 39:1515
3. Li J, Wahi RP, Chen H, Chen W, Wever H (1993) Z Metallkunde 84:268
4. Li J, Wahi RP (1995) Acta Metall Mater 43:507
5. Wang Y, Mukherji D, Chen W, Kutter T, Wahi RP, Wever H (1995) Z Metallkunde 86:365
6. Bettge D, Osterle W, Ziebs J (1995) Z Metallkunde 86:190
7. Jiao F, Zhu J, Wahi RP, Chen H, Chen W, Wever H (1992) In: Rie KT (ed) Proc. Conf. LCF and Elasto-Plastic Behavior of Materials, Elsevier Applied Science, London, p 298
8. Balikci E, Raman A, Mirshams RA (1997) Metall Mater Trans A 28A:1993
9. Balikci E, Mirshams RA, Raman A (1999) Z Metallkunde 90:132
10. Balikci E, Ferrell RE Jr, Raman A (1999) Z Metallkunde 90:141
11. Balikci E, Raman A, Mirshams RA (1999) Metall Mater Trans A 30A:2803
12. Balikci E, Mirshams RA, Raman A (1999) Mater Sci Eng A 265A:50
13. Balikci E, Mirshams RA, Raman A (2000) J Mater Eng Perform 9:324
14. Balikci E (1998) Ph.D. dissertation "Microstructure evolution and its influence on the thermal expansion and tensile properties of the superalloy IN738LC at high temperatures", Louisiana State University, BR, LA, USA
15. Roy I, Balikci E, Ibekwe S, Raman A (2005) J Mater Sci 40:6207, doi: 10.1007/s10853-005-3154-6
16. Doherty RD (1982) Metal Sci 16:1
17. Voorhees PW, Johnson WC (1988) Phys Rev Let 61:2225
18. Davies CKL, Nash P, Stevens RN (1980) Acta Metall 28:179
19. Tsumuraya K, Miyata Y (1983) Acta Metall 31:437
20. Johnson WC, Voorhees PW, Zupon DE (1989) Metal Trans 20A:1175
21. Calderon HA, Voorhees PW, Murray JL, Kostorz G (1994) Acta Metall Mater 42:991
22. Wolfsdorf TL, Bender WH, Voorhees PW (1997) Acta Mater 45:2279
23. Ricks RA, Porter AJ, Ecob RC (1983) Acta Metall 31:43
24. Su CH, Voorhees PW (1996) Acta Mater 44:1987
25. Johnson WC, Voorhees PW (1987) J Appl Phys 61:1610
26. Johnson WC, Abinandanan TA, Voorhees PW (1990) Acta Metall Mater 38:1349
27. McCormack M, Khachaturyan AG, Morris JW (1992) Acta Metall Mater 40:325
28. Abinandanan TA, Johnson WC (1993) Acta Metall Mater 41:17
29. Wang Y, Chen LQ, Khachaturyan AG (1993) Acta Metall Mater 41:279
30. Socrate S, Parks DM (1993) Acta Metall Mater 41:2185
31. Abinandanan TA, Johnson WC (1993) Acta Metall Mater 41:27
32. Hort W, Johnson WC (1994) Metall and Mater Trans 25A:2695
33. Fahrmann M, Fratzl P, Paris O, Fahrmann E, Johnson WC (1995) Acta Metall Mater 43:1007
34. Wang Y, Khachaturyan AG (1995) Acta Metall Mater 43:1837
35. Huh JY, Johnson WC (1995) Acta Metall Mater 43:1631
36. Su CH, Voorhees PW (1996) Acta Mater 44:2001
37. Nabarro FRN, Cress CM, Kotschy P (1996) Acta Mater 44:3189
38. Gurtin ME, Voorhees PW (1996) Acta Mater 44:235
39. Svoboda J, Lukas P (1996) Acta Mater 44:2557
40. Johnson WC (1997) Metall Mater Trans 28A:27
41. Mou Y, Howe JM (1997) Metall Mater Trans 28A:39
42. Mou Y, Howe JM (1997) Acta Mater 45:823
43. Li DY, Chen LQ (1997) Acta Mater 45:2435
44. Agarwal BD, Broutman LJ (1990) In: Analysis and performance of fiber composites, 2nd edn. John Wiley & Sons, Inc., New York, p 141